

Break-up mechanisms in heavy ion collisions at low energies

L. Shvedov^a, M. Colonna^a, M. Di Toro^{a,b}

^a*LNS-INFN, I-95123, Catania, Italy*

^b*Physics and Astronomy Dept. University of Catania, Italy*

We investigate reaction mechanisms occurring in heavy ion collisions at low energy (around 20 MeV/u). In particular, we focus on the competition between fusion and break-up processes (Deep-Inelastic and fragmentation) in semi-peripheral collisions, where the formation of excited systems in various conditions of shape and angular momentum is observed. Adopting a Langevin treatment for the dynamical evolution of the system configuration, described in terms of shape observables such as quadrupole and octupole moments, we derive fusion/fission probabilities, from which one can finally evaluate the corresponding fusion and break-up cross sections. The dependence of the results on shape, angular momentum and excitation energy is discussed.

PACS numbers: 25.70.-z, 25.70.Lm, 21.30.Fe, 24.60.Ky

I. INTRODUCTION

Nuclear reactions between medium-mass nuclei at low energies (around 20 MeV/u) offer the possibility to investigate several aspects of dissipative mean-field dynamics and to probe nuclear matter under extreme conditions with respect to shape, spin and excitation energy. In this energy domain, well above the Coulomb barrier but below the Fermi energies, one essentially observes two types of reaction mechanisms: Fusion dominates in the case of central and semi-peripheral collisions, while binary re-separation processes, associated with deep-enelastic or fast fission mechanisms, essentially involve the remaining range of (semi-)peripheral reactions [1]. However, along the transition from fusion to binary processes, composite systems with rather elongated shape and large intrinsic angular momentum can be formed, corresponding to metastable (or even unstable) conditions, where mean-field fluctuations may play a decisive role in determining the final outcome. The presence of large event by event variances related to the onset of new instabilities have been already noted in experiments, from the anomalous distribution of primary fragment properties in binary events [2, 3]. The observed variances (in mass, charge, excitation energy, angular distribution) appeared much larger than the ones predicted by mean-field nucleon exchange models. Similar conclusions were reached in theory simulations based on stochastic transport models [4].

Interaction times are quite long and a large coupling among various mean-field modes is expected, leading to a co-existence of the different reaction mechanisms in semi-central collisions. The study of the competition between fusionlike and binarylike processes and, more generally, of the fate of the hot nuclear residues created in these reactions is a longstanding problem, from which one can learn a lot about mean-field dynamics and fundamental properties of nuclear forces. This issue has recently found a renewed interest, due to the possibility to perform new analyses involving neutron-rich or even exotic systems [5]. In these conditions the reaction mechanism

characterizing dissipative collisions is expected to be sensitive to the density dependence of the isovector part of the nuclear interaction, a matter that is largely debated nowadays [5, 6].

In reactions involving medium-heavy nuclei, as a result of the complex neck dynamics, one can also observe, in sufficiently inelastic collisions, new modes of re-separation of the colliding system, such as dynamical ternary breaking, with massive fragments nearly aligned along a common separation axis [7, 8]. Experimental evidences of this mechanism have been recently reported in the case of $^{197}\text{Au} + ^{197}\text{Au}$ collisions at 15 MeV/u, where also aligned quaternary breaking has been observed [9]. These effects could still be explained in terms of the persistence of the excitation of shape and rotational modes in the projectile-like(PLF) and/or target like(TLF) fragments that are formed in binarylike events, that would lead to further re-separation along a preferential axis, similarly to what happens in fast-fission processes of PLF or TLF. It is worth mentioning that, at higher beam energy (around 40 MeV/u), where apart from mean-field effects two-body correlations are important, ternary breakings become the dominant process and new features are observed, corresponding to the emission of small fragments coming directly from the strongly interacting neck region [10]. Actually one may think in terms of a smooth transition between the different decay modes of PLF and/or TLF, from fast fission, characterized by the splitting into fragments with similar size and small relative velocity, to neck emission, where small fragments are emitted with larger relative velocity with respect to PLF and TLF.

From the above discussion, it is clear that the understanding of the competition between reaction mechanisms in dissipative collisions, as well as of the nature of new exotic re-separation modes, requires a thorough analysis of the underlying mean-field dynamics and associated shape fluctuations and rotational effects. In this paper, we attempt to improve the dynamical description of low energy collisions by coupling a microscopic transport approach based on mean-field concepts, suitable to follow the early stage of the collision up to the formation

of composite excited sources, to a more refined treatment of the dynamics of shape observables, including the associated fluctuations within the Langevin scheme [11], for the following evolution up to the definition of the final outcome. In particular, we will discuss the dynamics of excited sources characterized by given values of quadrupole and octupole moments and intrinsic angular momentum. This allows one to investigate the competition between fusionlike and binarylike reaction mechanisms and to evaluate fusion cross sections, as well as the probability and the features of fast-fission processes of PLF (or TLF). The paper is organized as it follows: In Section 2 we present the hybrid transport treatment employed to follow the dynamical evolution of the system. Results concerning the competition between fusion and binary processes are discussed in Section 3. Finally conclusions and perspectives are drawn in Section 4.

II. SIMULATION OF THE COLLISIONAL DYNAMICS

A. Dynamical description of nuclear reactions

The evolution of systems governed by a complex phase space can be described by a transport equation, of the Boltzmann-Nordheim-Vlasov (BNV) type, with a fluctuating term, the so-called Boltzmann-Langevin equation (BLE) [12, 13]:

$$\frac{df}{dt} = \frac{\partial f}{\partial t} + \{f, H\} = I_{coll}[f] + \delta I[f], \quad (1)$$

where $f(\mathbf{r}, \mathbf{p}, t)$ is the one-body distribution function, or Wigner transform of the one-body density, $H(\mathbf{r}, \mathbf{p}, t)$ the mean field Hamiltonian, I_{coll} the two-body collision term (that accounts for the residual interaction) incorporating the Fermi statistics of the particles, and $\delta I[f]$ the fluctuating part of the collision integral. The nuclear EOS, directly linked to the mean-field Hamiltonian H , can be written as:

$$E/A(\rho, I) = E_s/A(\rho) + C_{sym}(\rho)I^2 + O(I^4), \quad (2)$$

where $I = (N - Z)/A$ is the asymmetry parameter. We adopt a soft isoscalar EOS, $E_s/A(\rho)$, with compressibility modulus $K = 200 \text{ MeV}$, which is favored e.g. from flow studies [14]. For the density (ρ) dependence of the symmetry energy, $C_{sym}(\rho)$, we consider a linear increase of the potential part of the symmetry energy with density (asystiff):

$$C_{sym}(\rho) = a \cdot \left(\frac{\rho}{\rho_0}\right)^{2/3} + b \cdot (\rho/\rho_0), \quad (3)$$

where ρ_0 is the saturation density, $a=13.4 \text{ MeV}$ and $b=18 \text{ MeV}$. From the expression of the energy density, Eq.(2), the mean-field potential is directly derived. The free energy- and angle-dependent nucleon-nucleon cross section is used in the collision integral [15].

Within such approach, the system is described in terms of the one-body distribution function f , but this function may experience a stochastic evolution in response to the action of the fluctuating term $\delta I[f]$.

However, the numerical resolution of the full BL equation is not available yet in 3D. Approximate treatments to the BLE have been introduced so far, see Refs.[15, 16], such as the Stochastic Mean Field (SMF) model, that consists in the implementation of stochastic density fluctuations only in coordinate space and can be solved numerically using the test particle method [15]. The latter approach has shown to be particularly appropriate for the description of the evolution of the dilute unstable sources that develop in dissipative collisions at Fermi energies (30-100 MeV/u) [17]. However, here we are essentially interested in semi-central reactions at lower energies where, most likely, the formation of elongated (rather than dilute) systems is observed, and phenomena associated with surface (rather than volume) metastability and/or instability may take place. To improve the treatment of fluctuations suitable to describe the latter scenario, we will adopt a hybrid description of the dynamics: We follow the microscopic SMF evolution until the time instant when local thermal equilibrium is established and one observes the formation of quasi-stationary elongated systems, with density close to the normal value. Then, to deal with the following evolution of the system, we move to a more macroscopic model description, where the system is characterized in terms of global observables, for which the full treatment of fluctuations in phase space is numerically affordable, as explained below.

B. Dynamical evolution of shape observables

This Section is devoted to the description of the dynamical evolution of excited systems whose leading degrees of freedom are shape observables, while the density keeps always close to the normal value, $\rho_0 = \frac{3}{4\pi r_0^3}$, being r_0 the nuclear radius constant ($r_0 = 1.2 \text{ fm}$). The configuration of the system under study, having given charge Z and mass A , is described by three global observables (and associated velocities): the quadrupole moment β_2 , the octupole moment β_3 and the rotation angle ω . For situations far from the spherical shape the thermal agitation can induce fluctuations that may eventually lead to break-up channels. Hence the correct treatment of shape fluctuations is crucial for the characterization of the reaction mechanism. To this purpose, we consider the stochastic extension of the Rayleigh-Lagrange equations of motion [18] (the Langevin equation):

$$\frac{d}{dt} \frac{\partial L}{\partial \dot{q}_i} + \frac{\partial F}{\partial \dot{q}_i} = \frac{\partial L}{\partial q_i} + F_{fluc}(t), \quad (4)$$

where $q_i (i = 1, 2, 3) = (\omega, \beta_2, \beta_3)$. $L(q_i, \dot{q}_i) = E_{kin}(q_i, \dot{q}_i) + E_{rot}(q_i, \dot{q}_i) - E_{pot}(q_i)$ denotes the La-

grangian of the system and

$$F(q_i, \dot{q}_i) = \frac{1}{2} \frac{dE_{tot}}{dt} = \frac{1}{2} \sum_{i,j=2}^3 R_{ij} \dot{q}_i \dot{q}_j \quad (5)$$

is the Rayleigh dissipation function. E_{kin} , E_{rot} and E_{pot} indicate the kinetic, rotational and potential energy of the system, respectively, and the quantity R_{ij} is the dissipation tensor. The difference with respect to the standard Rayleigh-Lagrange equations is the fluctuation term F_{fluc} , that can be interpreted as a rapidly fluctuating stochastic force, in the same spirit of the Brownian motion, similar to the fluctuating term of the BLE, Eq.(1). We solve numerically the set (4) of coupled equations.

For given values of the quadrupole and octupole moments, the shape of the system is parametrized, in terms of the polar angle θ , as it follows:

$$R(\theta) = R_0(\beta_2, \beta_3) \{1 + \beta_1(\beta_2, \beta_3) Y_{10}(\theta) + \beta_2 Y_{20}(\theta) + \beta_3 Y_{30}(\theta)\}, \quad (6)$$

where the functions $Y_{l0}(\theta)$ are spherical harmonics. The parameters β_1 and R_0 are introduced to conserve the position of the center of mass and the total volume V of the system and can be determined from the equations:

$$\int dV z = \frac{2\pi}{4} \int_0^\pi R^4(\theta) \sin \theta \cos \theta d\theta = 0, \quad (7)$$

$$\int dV = \frac{2\pi}{3} \int_0^\pi R^3(\theta) \sin \theta d\theta = \frac{4}{3} \pi r_0^3 A, \quad (8)$$

where z denotes the coordinate along the system maximum elongation axis (or symmetry axis). In the following we discuss in detail the derivation of the different terms of the Lagrangian L .

1. Rotational energy

The rotational energy is simply equal to:

$$E_{rot} = \frac{1}{2} I(\beta_2, \beta_3) \dot{\omega}^2, \quad (9)$$

where

$$I(\beta_2, \beta_3) = \frac{\pi m \rho_0}{5} \int_0^\pi R^5(\theta) \{1 + \cos^2 \theta\} \sin \theta d\theta \quad (10)$$

is the moment of inertia for the whole system, being m the nucleon mass.

2. Kinetic energy

The kinetic energy can be expressed as it follows:

$$E_{kin} = \frac{1}{2} \sum_{i,j=2}^3 M_{ij}(\beta_2, \beta_3) \dot{q}_i \dot{q}_j \quad (11)$$

To calculate the mass tensor M_{ij} , we adopt the prescriptions of Ref.[19]:

$$M_{i,j} = \frac{1}{2} (M'_{i,j} + M'_{j,i}) \quad (12)$$

with

$$M'_{i,j} = 2\pi m \rho_0 \int_0^\pi \sum_{l=1}^L b_{il} R^{l+2}(\theta) P_l(\cos \theta) \left\{ \frac{\partial R_0}{\partial \beta_j} S + R_0 \left(\frac{\partial \beta_1}{\partial \beta_j} Y_{10} + Y_{j0} \right) \right\} \sin \theta d\theta. \quad (13)$$

Here P_l are Legendre polynomials and $S(\theta) = \frac{R(\theta)}{R_0}$. In our calculations we have $L = 5$. The coefficients b_{2l} and b_{3l} are obtained solving the system of equations:

$$\sum_{l=1}^L A_{kl} b_{ml} = C_{mk} \quad k = 1 \dots L, \quad m = 2, 3 \quad (14)$$

with

$$A_{kl} = \int_0^\pi R^{l-1}(\theta) \left\{ l P_l(\cos \theta) - \frac{1}{R(\theta)} \frac{\partial R(\theta)}{\partial \theta} \frac{\partial P_l(\cos \theta)}{\partial \theta} \right\} \cdot R^{k-1}(\theta) \left\{ k P_k(\cos \theta) - \frac{1}{R(\theta)} \frac{\partial R(\theta)}{\partial \theta} \frac{\partial P_k(\cos \theta)}{\partial \theta} \right\} \sin \theta d\theta, \quad (15)$$

$$C_{mk} = \int_0^\pi R^{k-1}(\theta) \left\{ k P_k(\cos \theta) - \frac{1}{R(\theta)} \frac{\partial R(\theta)}{\partial \theta} \frac{\partial P_k(\cos \theta)}{\partial \theta} \right\} \cdot \left\{ \frac{\partial R_0}{\partial \beta_m} S + R_0 \left(\frac{\partial \beta_1}{\partial \beta_m} Y_{10} + Y_{m0} \right) \right\} \sin \theta d\theta. \quad (16)$$

3. Potential energy: Nuclear term

Concerning the nuclear part of the potential energy, E_n , we discuss essentially the surface contribution, since our system keeps a volume constant in time. We adopt a double volume integral of the Yukawa-plus-exponential folding function [20]:

$$E_n = -\frac{a_s(1 - k_s I^2)}{8\pi^2 r_0^2 a^3} \int_V \int_V \left(\frac{\sigma}{a} - 2 \right) \frac{e^{-\sigma/a}}{\sigma} d^3 r d^3 r', \quad (17)$$

where a_s is the surface-energy constant, k_s is the surface-asymmetry constant and a is the range of the Yukawa-plus-exponential potential. σ denotes the modulus of the relative distance $\sigma = |r - r'|$. Parameters have been fitted to the ground-state energies and fission barrier heights [21, 22]. In order to reduce the numerical efforts, the integral of Eq.(17) can be transformed into a double surface integral, by using the twofold Gauss divergence theorem. For axially symmetric shapes, one of the azimuthal

integrations can be performed trivially [20, 23] and the resulting threefold integral is:

$$E_n = \frac{a_s(1 - k_s I^2)}{4\pi r_0^2} \iiint \left\{ 2 - \left[\left(\frac{\sigma}{a} \right)^2 + 2\frac{\sigma}{a} + 2 \right] e^{-\sigma/a} \right\} \\ \times \frac{P(\theta, \theta', \phi) P(\theta', \theta, -\phi)}{\sigma^4} d\theta d\theta' d\phi, \quad (18)$$

where the distance σ can be expressed as:

$$\sigma = [R^2(\theta) + R^2(\theta') - 2R(\theta)R(\theta') \\ \cdot \{\cos\theta \cos\theta' + \sin\theta \sin\theta' \cos\phi\}]^{1/2}$$

and

$$P(\theta, \theta', \phi) = R(\theta) \sin\theta \{R^2(\theta) - R(\theta)R(\theta') [\cos\theta \cos\theta' + \\ + \sin\theta \sin\theta' \cos\phi] - R(\theta') \frac{\partial R(\theta)}{\partial \theta} [\sin\theta \cos\theta' - \cos\theta \sin\theta' \cos\phi]\} \\ \times \left\{ R_0 \left\{ \frac{\partial \beta_1}{\partial \beta_i} Y_{10} + Y_{i0} \right\} + \frac{\partial R_0}{\partial \beta_j} S \right\} R^2(\theta) \sin\theta d\theta \quad (23)$$

4. Potential energy: Coulomb term

The Coulomb part of the potential energy is taken as [24]:

$$E_C = E_C^{sharp} + \Delta E_C^{dif}$$

where E_C^{sharp} is the Coulomb energy corresponding to a sharp charge density distribution and ΔE_C^{dif} is a correction due to the diffuseness.

The sharp-surface part of the Coulomb energy is equal to:

$$E_C^{sharp} = -\frac{\rho_p^2 \pi}{6} \iiint \frac{P(\theta, \theta', \phi) P(\theta', \theta, -\phi)}{\sigma} d\theta d\theta' d\phi \quad (19)$$

where ρ_p is the charge(proton) density, $\rho_p = \frac{Z}{A} \rho_0$. The correction to the Coulomb energy due to the diffuseness can be expressed as:

$$\Delta E_C^{dif} = \rho_p^2 \pi a_C^3 \iiint \left\{ 2\frac{\sigma}{a_C} - 5 + \left[\frac{1}{2} \left(\frac{\sigma}{a_C} \right)^2 + 3\frac{\sigma}{a_C} + 5 \right] e^{-\sigma/a_C} \right\} \\ \frac{P(\theta, \theta', \phi) P(\theta', \theta, -\phi)}{\sigma^4} d\theta d\theta' d\phi, \quad (20)$$

where a_C is the range parameter of the Yukawa function generating the diffuse charge distribution [23–25].

5. Dissipation function

The one-body dissipation mechanism is evaluated as it follows (see Ref.[18] for details):

$$\frac{dE}{dt} = m\rho_0 \bar{v} \oint \dot{n}^2 dS \quad (21)$$

where the integration is performed over the whole surface of the system, $\bar{v} = \frac{3}{4} v_F$ is the average nucleon velocity and

$$\dot{n}^2 = \frac{\left| \frac{\partial \mathcal{R}}{\partial t} \right|^2}{|\nabla \mathcal{R}|^2}, \quad \mathcal{R} = r - R(\theta) \quad (22)$$

Hence we get the following expressions for the dissipation tensor R_{ij} :

$$R_{i,j} = 2^{|i-j|} \pi m \rho_0 \bar{v} \\ \times \int_0^\pi \frac{\left\{ R_0 \left\{ \frac{\partial \beta_1}{\partial \beta_i} Y_{10} + Y_{i0} \right\} + \frac{\partial R_0}{\partial \beta_i} S \right\}}{1 + \frac{1}{R^2(\theta)} \left\{ \frac{\partial R(\theta)}{\partial \theta} \right\}^2} \\ \times \left\{ R_0 \left\{ \frac{\partial \beta_1}{\partial \beta_j} Y_{10} + Y_{j0} \right\} + \frac{\partial R_0}{\partial \beta_j} S \right\} R^2(\theta) \sin\theta d\theta \quad (23)$$

6. The Langevin term

The stochastic force $F_{fluc}(t)$ will determine fluctuations in momentum space, according to the value of the diffusion coefficient D . We assume that

$$\langle F_{fluc}(t) F_{fluc}(t+s) \rangle = D \delta(s) \quad (24)$$

The action of the stochastic force F_{fluc} may be simulated numerically by repeatedly producing a random kick δP in the collective velocity associated with the quadrupole and octupole moments. The value of δP is chosen randomly from a Gaussian distribution with mean value and variance given by:

$$\overline{\delta P} = 0 \quad (25)$$

$$\overline{(\delta P)^2} = D \delta t \quad (26)$$

where δt is the small time step between two kicks. The diffusion coefficient D can be found using the Einstein relation:

$$D = 2T\gamma, \quad (27)$$

where γ is the dissipation coefficient and T is the temperature of the system [26]. Hence the fluctuations that we are considering are induced essentially by the thermal agitation. We notice that our dissipation tensor R_{ij} , introduced above, has also nondiagonal terms. Hence, to correctly extract the dissipation coefficients, we diagonalize the dissipation tensor $R_{ij} \rightarrow \gamma_{ij}$. The tensor γ_{ij}

will have only diagonal elements: γ_2 and γ_3 . Now we can find D_2 and D_3 in the new coordinate system and evaluate δP_2 and δP_3 , the random kicks for the new coordinates. Finally it is possible to go back to the general coordinates β_2 and β_3 , by the inverse transformation, and obtain δP_{β_2} and δP_{β_3} .

III. RESULTS

We will exploit the Langevin treatment outlined above to investigate the competition between (incomplete) fusion and binary break-up mechanisms in low energy reactions. We consider the system $^{36}\text{Ar} + ^{96}\text{Zr}$ at two beam energies, 9 and 16 MeV/u, in the following range of impact parameters: $b = 5\text{-}7$ fm and $b = 4\text{-}6$ fm at 9 and 16 MeV/u, respectively. Within this selection, according to the SMF dynamical evolution, one observes the formation of rather elongated configurations for which fluctuations are expected to be crucial in determining the following evolution. For lower impact parameters, the conditions of the reactions are such that one always obtains incomplete fusion, while for larger impact parameters binary break-up is observed. Contour plots of the density in the reaction plane, as obtained in the SMF calculations, are displayed in Figs.1-2, for the two reactions.

The description of the system in terms of the global observables β_2 , β_3 and ω begins at the moment when, according to the full SMF evolution, the composite system reaches a quasi-stationary shape, having dissipated almost completely the radial part of the kinetic energy deposited into the system, while the angular part is converted into intrinsic spin. This time instant is estimated to be around $t_{freeze-out} \approx 200$ fm/c. During the earlier dynamical evolution, pre-equilibrium nucleon emission takes place. As a consequence, mass and charge of the system are smaller than the total mass and charge numbers, respectively. We get $A \approx 122$, $Z \approx 53$. As one can see from Figs.1-2, the system configuration can be suitably parametrized in terms of quadrupole and octupole moments. From this point of view, the Langevin treatment introduced above appears appropriate to describe the following evolution, though the dynamical description is devolved to few leading degrees of freedom. The initial conditions of the Langevin equation have been determined running 10 SMF trajectories. The corresponding parameters are listed in Tables I-II, for a couple of events, for each considered case.

Then, within the Langevin treatment, 200 stochastic events were considered for each SMF trajectory. Fluctuations are injected each 3 fm/c.

According to the values listed in Tables I-II, we test essentially the behavior of composite systems with a variety of conditions of angular momentum, ranging from 50 \hbar to 100 \hbar and quadrupole moment β_2 , from 0.2 to 1. The excitation energy is about 250 MeV, corresponding to temperatures of the order of 4 MeV. Apart from

b (fm)	E^* (MeV)	L (\hbar)	β_2	β_3	$\frac{d\beta_2}{dt}$	$\frac{d\beta_3}{dt}$	P
7	225	100	1.14	-0.73	0.099	0.024	0.990
7	242	95	1.00	-0.76	0.143	-0.129	0.990
6	240	77	0.83	0.47	0.062	-0.010	0.645
6	224	84	1.01	-0.52	0.113	-0.063	0.880
5	216	64	0.58	-0.32	0.125	0.938	0.375
5	227	58	0.56	0.36	-0.004	0.005	0.145

TABLE I: Characteristics of the composite system, as obtained in the reaction $^{36}\text{Ar} + ^{96}\text{Zr}$ at 9 MeV/u at the time $t_{freeze-out}$: Excitation energy, intrinsic angular momentum, quadrupole moment, octupole moment and associated collective velocities. The time unit adopted to define the collective velocities is $10^{-22}\text{s} = 30$ fm/c. Two events are displayed for each impact parameter. The fission probability (see text) is reported in the last column.

b (fm)	E^* (MeV)	L (\hbar)	β_2	β_3	$\frac{d\beta_2}{dt}$	$\frac{d\beta_3}{dt}$	P
6	279	90	0.88	0.34	0.016	0.059	1.000
6	277	97	0.88	0.44	-0.015	-0.031	1.000
5	241	73	0.37	0.15	-0.063	-0.047	0.320
5	252	77	0.63	0.40	0.136	-0.020	0.580
4	258	63	0.31	0.06	0.052	0.018	0.110
4	247	52	0.22	0.05	-0.007	0.002	0.035

TABLE II: Same as in Table I, but for the reaction at 16 MeV/u.

the situation observed in the case of $b = 7$ fm, $E/A = 9$ MeV/u, the octupole moment, β_3 , always takes rather small values, of both signs, indicating that the memory of the entrance channel mass asymmetry is lost. Also the quadrupole and octupole collective velocities are rather small and may take values of both signs, suggesting that collective motions, apart from the rotation associated with the intrinsic spin, are damped. These conditions correspond closely to quasi-stationary, metastable situations, i.e. the system is stable against small shape fluctuations. From one side, it may evolve radiating its excitation energy and spin and relaxing slowly towards the spherical configuration. On the other hand, if the amplitude of the kicks of the associated collective velocities is large enough, the system may overcome the fission barrier and reach configurations corresponding to surface instabilities, from which it rapidly separates in two pieces. However, one should also consider that the latter possibility is in competition with nucleon emission, that reduces the excitation energy (and the associated amplitude of thermal fluctuations), while the shape of the system is evolving. The nucleon emission rate can be evaluated according to the standard Weisskopf formalism [27]. For the situations under study, the excitation energy reduces, due to nucleon emission, approximately by 2.5 MeV each 30 fm/c. We follow the trajectory of the system until the available excitation energy is fully dissipated.

Hence, thanks to the introduction of fluctuations in

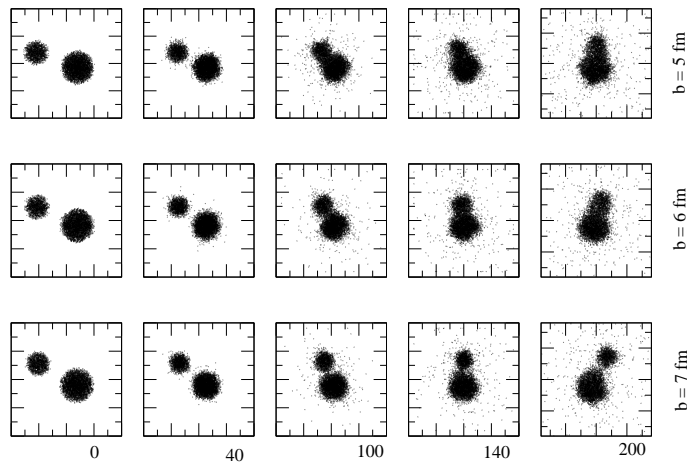


FIG. 1: Contour plots of the density projected on the reaction plane calculated with SMF for the reaction $^{36}\text{Ar} + ^{96}\text{Zr}$ at 9 MeV/u, at several times (fm/c). The size of each box is 40 fm.

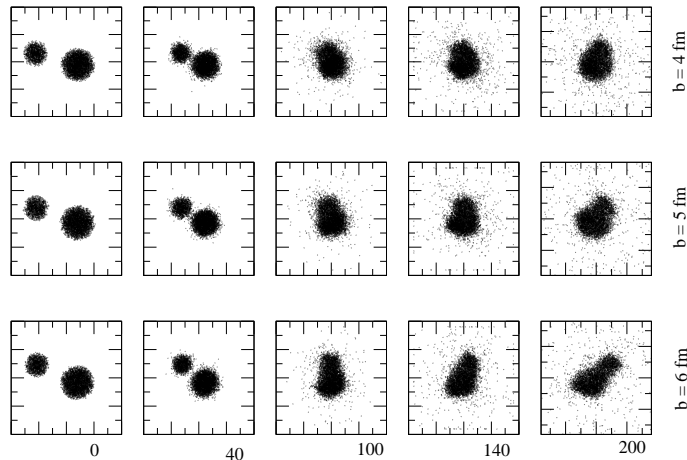


FIG. 2: The same as in Fig. 1 but at 16 MeV/u.

the dynamical evolution, for a given impact parameter one observes a bifurcation of trajectories, leading either to compact shapes (fusion) or to elongated shapes, with large values of quadrupole and/or octupole moments, that eventually cause the break-up of the system. Actually the two possible outcomes are associated with a kind of bimodal behavior of the shape observables, related to configurations corresponding to local minima of the total (surface + Coulomb) energy. It may be interesting to notice that bimodality has been recently observed also in the context of liquid-gas phase transitions, where volume instabilities are concerned and dilute systems may either recompact to normal density or split into a huge number of small fragments [28].

A. Fission rates

In the following, we will first discuss some illustrative results obtained in the case of the reaction at 16 MeV/u, $b = 5-6$ fm. In Fig.3 we present one example of trajectories corresponding to the two possible exit channels (fusion or fission), in the (β_2, β_3) plane. Due to the random kicks, starting from the same initial conditions, rather different paths are explored. It should be noticed that, also in the case of trajectories leading to fusion, the final configuration is not exactly spherical, but is associated with small (not vanishing) values of the quadrupole moment. This corresponds to the stationary configuration compatible with the amount of intrinsic angular momentum present in the system. On the other hand, break-up configurations are characterized by rather large values of

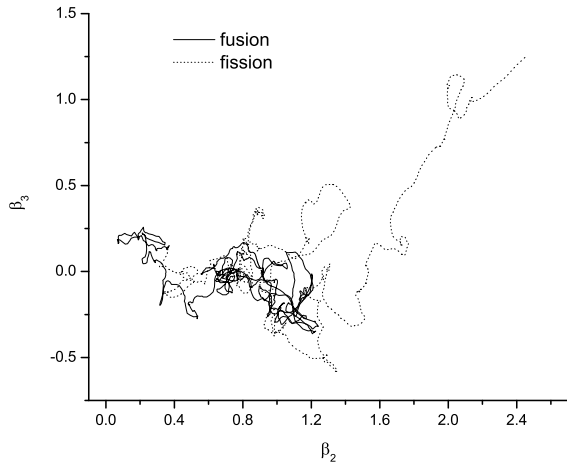


FIG. 3: One example of trajectories leading either to fusion or to break-up, in the (β_2, β_3) plane, as obtained in the reaction at 16 MeV/u, $b = 5$ fm.

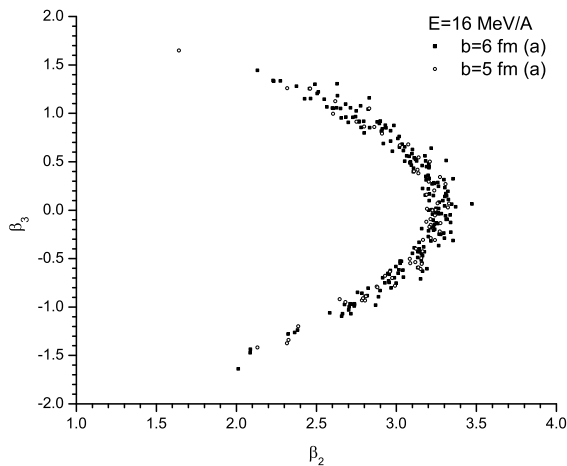


FIG. 4: Correlations between the values of quadrupole and octupole moments, as obtained for the break-up configurations in the case of the reaction at 16 MeV/u, $b = 5-6$ fm.

β_2 and/or β_3 . Actually one sees an interesting correlation between the two parameters, that is represented in Fig.4. In fact, both a large quadrupole or octupole moments are linked to break-up configurations, that correspond to tangent spheroids. Fluctuations of the octupole moment are rather large, though the majority of the events is located near $\beta_3 = 0$, corresponding to symmetric fission.

In Figs.5-6 (left) the fission rate, dN/dt , as obtained for $b = 6-7$ fm at 9 MeV/u and $b = 5-6$ fm at 16 MeV/u, is displayed as a function of time for a set of 200 events in each of the cases considered. For the most peripheral impact parameters, after an initially increasing trend, re-

lated to the time interval needed to build and propagate fluctuations, we observe an almost exponential decrease, as expected in the case of constant break-up probability γ_{break} . In this case one can write: $dN/dt = N_t \gamma_{break}$, with $N_t = N_0 e^{-\gamma_{break} t}$ and $N_0 = 200$ (the total number of events considered). This corresponds to situations where the break up probability ($\gamma_{break} \approx 0.002$ c/fm) is not much affected by the competing nucleon emission. All events practically lead to fission over a time interval that is shorter than the one needed to exhaust the available excitation energy by nucleon emission. In fact, the maximum of the emission rate is observed at about 300 fm/c and the system needs, on average, roughly 500 fm/c to reach the break-up configuration (this is actually the half life time $\tau_{break} = 1/\gamma_{break}$). On the other hand, for smaller impact parameters (corresponding to lower deformation of the system and lower angular momentum), the break-up probability γ_{break} is quenched approximately by a factor 4 (see the left panel of Figs.5-6) and decreases in the course of time because of nucleon emission, that reduces the excitation energy and the corresponding amount of thermal fluctuations. In most cases, the excitation energy deposited into the system is dissipated before the break up configuration may be reached. It is interesting to notice that, even in the most favourable case, the typical times of the process are rather large (500 fm/c), as compared for instance to the time scales associated with the development of volume instabilities in multifragmentation processes at higher energies (about 150 fm/c). This can be explained in terms of the larger amount of excitation energy deposited into the system in the latter case (that induces fluctuations of higher amplitude and collective radial expansion) and of the smaller growth times associated with volume instabilities [17].

The corresponding fraction of events that undergo break-up, P_{break} , is reported in Table I-II, at the two energies and for all impact parameters considered. From the estimated break-up probabilities it is possible to construct the fusion cross-section, $\sigma_f(b) = (1 - P_{break}) 2\pi b db$, that is displayed in Fig.7, for the two energies. We also show, for comparison, the results obtained within the SMF approach only, where due to the approximate treatment of fluctuations, one gets distributions close to a sharp cut-off (approximated by a sharp cut-off in the figure). It is interesting to notice that, especially in the case of the reaction at 9 MeV/u, the fusion cross section is reduced significantly by the introduction of fluctuations that, in turn, help the system to overcome the fission barrier and to break-up.

B. Features of fission fragments

The time t_{break} , needed to reach the break-up configuration, is connected to other interesting features of the reaction dynamics, depending on the various entrance channel conditions. In fact, due to the intrinsic spin, the system rotates while its shape evolves according to

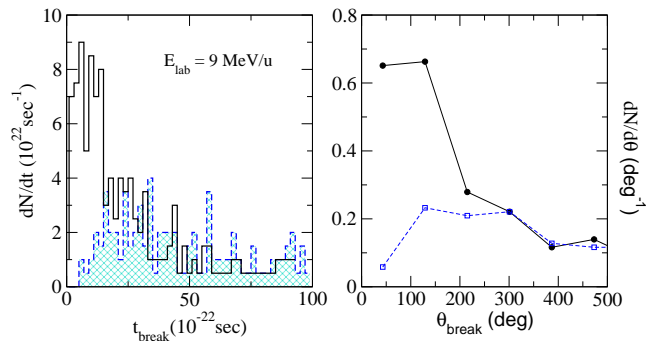


FIG. 5: (Color online) Left panel: Distribution of the time t_{break} (see text), as obtained for the reaction at 9 MeV/u and impact parameters $b = 7$ fm (full histogram) and $b = 6$ fm (shaded histogram). Right panel: Angular distribution of the break-up direction. Full line and circles refer to $b = 7$ fm; dashed line and open squares are for $b = 6$ fm.

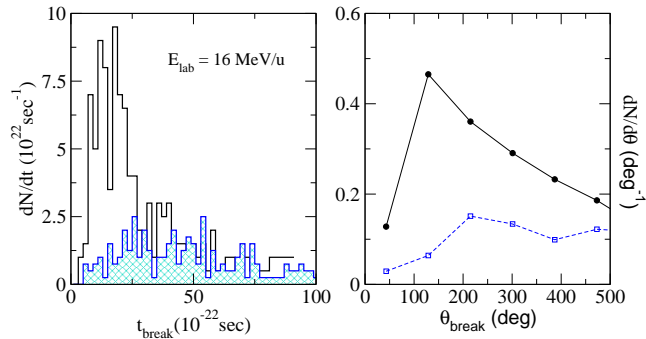


FIG. 6: (Color online) Same as Fig.5, for the reaction at 16 MeV/u and $b = 5-6$ fm.

Eq.(4). As a consequence, the direction along which the system separates into pieces is strictly connected to t_{break} . Hence the shape of the angular distribution of fission fragments can be used as a clock of the collision, from which one can extract information on the break-up probability and the underlying reaction mechanism. This is an appealing issue that can be investigated also experimentally by looking at the angular distribution of the emerging reaction products and at the possible existence of alignment effects [9, 10]. In the case of a fast break-up (fast fission) the angular distribution should exhibit a peak: due to the elongated shape of the system, the emission is not isotropic. Along the separation process, fragments acquire velocities essentially due to the Coulomb repulsion, according to the Viola systematics, like in standard fission, but with a preferential emission axis. The distribution of the angle, θ_{break} , corresponding

to the rotation (on the plane perpendicular to the direction of the intrinsic spin of the system) until the break-up configuration is reached is shown in Figs.5-6 (right panel), for the two energies and two impact parameters. Obviously, the shape of this distribution depends on the fission probability, but also on the system angular velocity (that in turn depends on the intrinsic spin). In fact, in absence of rotation (vanishing spin) the fragments would always be emitted along a fixed axis. In the case of the most peripheral events, a clear peak is observed in the distribution. On the other hand, for more central impact parameters, the half life time is much larger and one essentially gets a flat distribution for θ_{break} , similarly to what is expected in the case of standard statistical fission.

C. Fast-fission of PLF and TLF

Several shape, angular momentum and excitation energy conditions can be observed also, in the case of collisions between heavy systems, after the separation into PLF and TLF, for one (or both) of these products. Thus it is interesting to investigate fast fission processes of these objects, leading to ternary (or quaternary) breaking of the whole system. For instance, we display in Fig.8, density contour plots as obtained in SMF simulations of semi-peripheral collisions of Au + Au at 15 MeV/u, for which aligned ternary and quaternary breaking has been recently observed experimentally [9]. One can see that similar shape configurations, as the ones observed in the reactions investigated above, may appear for PLF/TLF fragments. However, these fragments have lower angu-

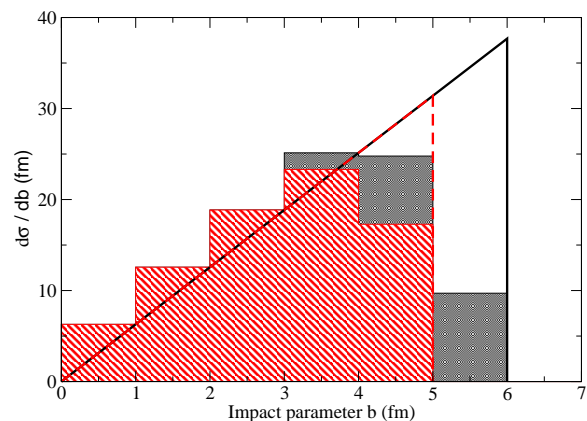


FIG. 7: (Color online) Fusion cross section, as a function of the impact parameter b , as obtained in the reactions at 9 MeV/u (black histogram) and 16 MeV/u (grey histogram) with the Langevin treatment, Eq.(4). The lines correspond to SMF simulations at 9 MeV/u (full) and 16 MeV/u (dashed).

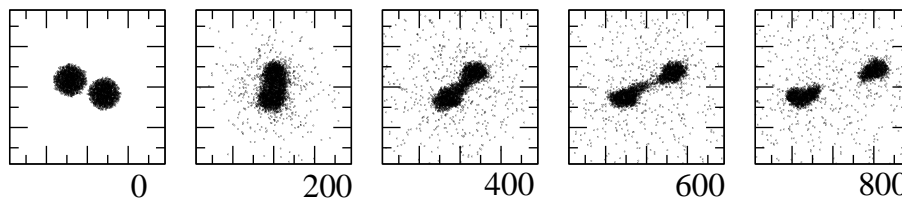


FIG. 8: Contour plots of the density projected on the reaction plane calculated with SMF for the reaction $^{197}\text{Au} + ^{197}\text{Au}$ at 15 MeV/u, $b = 6$ fm, at several times (fm/c). The size of each box is 80 fm.

lar momentum (about $20 - 40\hbar$) and excitation energy (of the order of 100 MeV). The corresponding break-up probability is of the order of 10% and emission times are longer (≈ 2000 fm/c). The fast-fission mechanism could explain qualitatively some of the features observed experimentally, such as alignment effects and fragment relative velocities and charge distributions. However, a thorough analysis of the kinematical properties of the reaction products [9], as well as the estimated rather short break-up times, suggests the persistence of non-equilibrium effects in momentum space, i.e. the presence of collective velocities in β_2 and/or β_3 , in addition to the tangential velocity generated by the intrinsic angular momentum. Collective velocities, probably underestimated in the SMF calculations, would speed up the fragmentation process since the system is pushed towards more exotic shapes, from which it is easier to overcome the fission barrier.

IV. CONCLUSIONS

In this article we have investigated the role of shape fluctuations in the dynamical evolution of excited systems that can be formed in semi-peripheral reactions at low energy (around 20 MeV/u). Quasi-stationary composite systems, with quadrupole and/or octupole deformation, are observed, for which shape fluctuations are essential to overcome the fission barrier and eventually break-up. This analysis is performed within a hybrid treatment that couples the study of the early stage of the dynamics, devolved to a microscopic stochastic transport approach, up to the formation of primary excited sources, to a full Langevin description of the leading degrees of

freedom of these objects: quadrupole, octupole moments and angular velocity. For temperature, shape and angular momentum conditions obtained in semi-peripheral reactions, typical time scales of the break-up process are of the order of 500 fm/c. The fission fragments are emitted along a preferential direction, that corresponds to the maximum elongation axis. Due to angular momentum effects, this direction may rotate while the shape of the system is evolving towards break-up configurations. Hence a careful analysis of the angular distribution of the reaction products may give relevant information about fission probabilities and the involved time scales, that in turn are closely linked to the mean-field dynamics and the properties of the nuclear interaction (range, surface energy, two-body correlations). From this study it is clear that a good treatment of mean-field fluctuations is a crucial point in the characterization of dissipative reactions. The model employed here provides a suitable description of surface modes, parametrized in terms of quadrupole and octupole oscillations, but it could miss some non-equilibrium effects that can help the system to break-up. In fact, collective velocities related to shape observables are likely underestimated in the SMF approach [29] and the role of multipoles higher than octupole is neglected in the Langevin treatment. A fully microscopic description of the whole process would be highly desirable, though it is far from being trivial. Some attempts are represented by improved quantum molecular dynamics calculations (ImQMD) [30]. Stochastic extensions of Time-Dependent-Hartree-Fock (TDHF) calculations should also provide a valuable tool to characterize reaction mechanisms in low energy collisions [31]. Work is in progress in this direction.

-
- [1] P.Lautesse et al., Eur. Phys. Jou. **A27**, 349 (2006)
 [2] T.C.Awes et al., Phys. Rev. Lett. **52**, 251 (1984)
 [3] V.Penumetcha et al., Phys. Rev. **C42**, 1489 (1990)
 [4] M.Colonna, M.Di Toro and A.Guarnera, Nucl. Phys. **A589**, 160 (1995)

- [5] F.Amorini et al., Phys. Rev. Lett. **102**, 112701 (2009)
 [6] V.Baran, M.Colonna, V.Greco, M.Di Toro, Phys. Rep. **410**, 335 (2005)
 [7] P.Glassel, D.v.Harrach, H.J.Specht, and L.Grodzins, Z.Phys. **A310**, 189 (1983)

- [8] A.A.Stefanini et al., Z. Phys. **A351**, 167 (1995)
- [9] I.Skwira-Chalot et al, Phys. Rev. Lett. **101**, 262701 (2008); J.Wilczynski et al., Phys. Rev. **C81**, 024605 (2010)
- [10] De Filippo et al., Phys. Rev. **C71**, 044602 (2005)
- [11] D.Boilley, E.Suraud, Y.Abe and S.Ayik, Nucl. Phys. **A556**, 67 (1993)
- [12] S.Ayik, C.Gregoire, Phys. Lett. **B212**, 269 (1988), and refs. therein.
- [13] J.Rizzo, P.Chomaz, M.Colonna, Nucl. Phys. **A806**, 40 (2008), and refs. therein
- [14] P. Danielewicz, R. Lacey, W.G. Lynch, Science **298**, 1592 (2002)
- [15] A.Guarnera, M.Colonna, Ph.Chomaz, Phys. Lett. **B373**, 297 (1996)
- [16] M. Colonna et al, Nucl. Phys. **A642**, 449 (1998)
- [17] P.Chomaz, M.Colonna, J.Randrup, Phys. Rep. **389**, 263 (2004)
- [18] J. Błocki, Y. Boneh, J.R. Nix, J. Randrup, M. Robel, A.J. Sierk, W.J. Świątecki, Ann. Phys. **113**, 330 (1978)
- [19] J.R. Nix, Ann. Phys. **41**, 52 (1967)
- [20] H.J. Krappe, J.R. Nix, A.J. Sierk, Phys. Rev. **C20**, 992 (1979)
- [21] P. Möller, J.R. Nix, Nucl. Phys. **A361**, 117 (1981)
- [22] P. Möller, J.R. Nix, Atomic Data and Nuclear Data Tables **39**, 213 (1988)
- [23] A.J. Sierk, Phys. Rev. **C33**, 2039 (1986)
- [24] K.T.R. Davies, J.R. Nix, Phys. Rev. **C14**, 1977 (1976)
- [25] W.D. Myers, Nucl. Phys. **A145**, 387 (1970)
- [26] L.D. Landau, E.M. Lifshitz, *Statistical Physics* Part 1. Vol. 5 (3rd ed.), Butterworth-Heinemann, ISBN 978-0-750-63372-7 (1980)
- [27] G.F. Bertsch, P.G. Reinhard, E.Suraud, Phys. Rev. **C53**, 1440 (1996)
- [28] E.Bonnet et al., Phys. Rev. Lett. **103**, 072701 (2009)
- [29] M.Colonna et al., Nucl. Phys. **A742**, 337 (2004)
- [30] Tian Jun-Long et al., Chinese Physics **C33**, 109 (2009)
- [31] K.Washiyama, S.Ayik, D.Lacroix, Phys. Rev. **C80**, 031602 (2009)